

Introduction

The objective is to develop experimental setups and to investigate liquid boiling processes in capillary-porous structures using optical methods [1]. Recent developments and future directions in flow visualization were reviewed in [2]. The authors note that over the past several decades, advances in experimental methods, visualization technologies, and computational techniques have substantially expanded the scope of observation – from classical approaches to more advanced methods such as high-speed imaging, laser-induced fluorescence, and digital holography.

The first gas laser is known to have been developed [3] using a mixture of helium and neon inert gases with high-frequency excitation of an electric discharge at a frequency of 30 MHz.

Subsequent experiments demonstrated the feasibility of DC pumping, as well as the existence of optimal parameter ranges [4]. For instance, the authors of [5] achieved an approximately two-fold increase (by a factor of ~ 1.75) in output power at a wavelength of 633 nm through combined DC and inductive (3 MHz) pumping of the LG-38 He-Ne laser.

Experimental setup

To visualize heat and mass transfer processes in the porous cooling system by photography, high-speed cinematography, and holographic interferometry, the heat exchange system was constructed from an alumina (corundum) tube with an outer diameter of 21×10^{-3} m. For power plant applications, single-, double-, and triple-layer mesh wicks with cell sizes of 0.4; 0.14×0.4 ; and $0.08 \times 0.14 \times 0.4$ mm, respectively, were used [1].

The heat source is a halogen quartz lamp KG-220-1000-3 positioned inside the tube, with the following principal specifications: voltage – 220 V; power – 1000 W; luminous flux – 26,000 lm; luminous efficacy – 26 lm/W; overall length – 0.18 m.

The notation in Fig. 1 is as follows: 1 – camera, 2 – viewfinder, 3 – tripod, 4 – lens, 5 – base plate, 6 – porous structure, 7 – alumina tube, 8 – lamp KG-220-1000-3, 9 – artery, 10 – stand, 11 – tube, 12 – bracket, 13 – locking screw, 14 – water, 15 – scale, 16 – tank, 17 – floodlight.

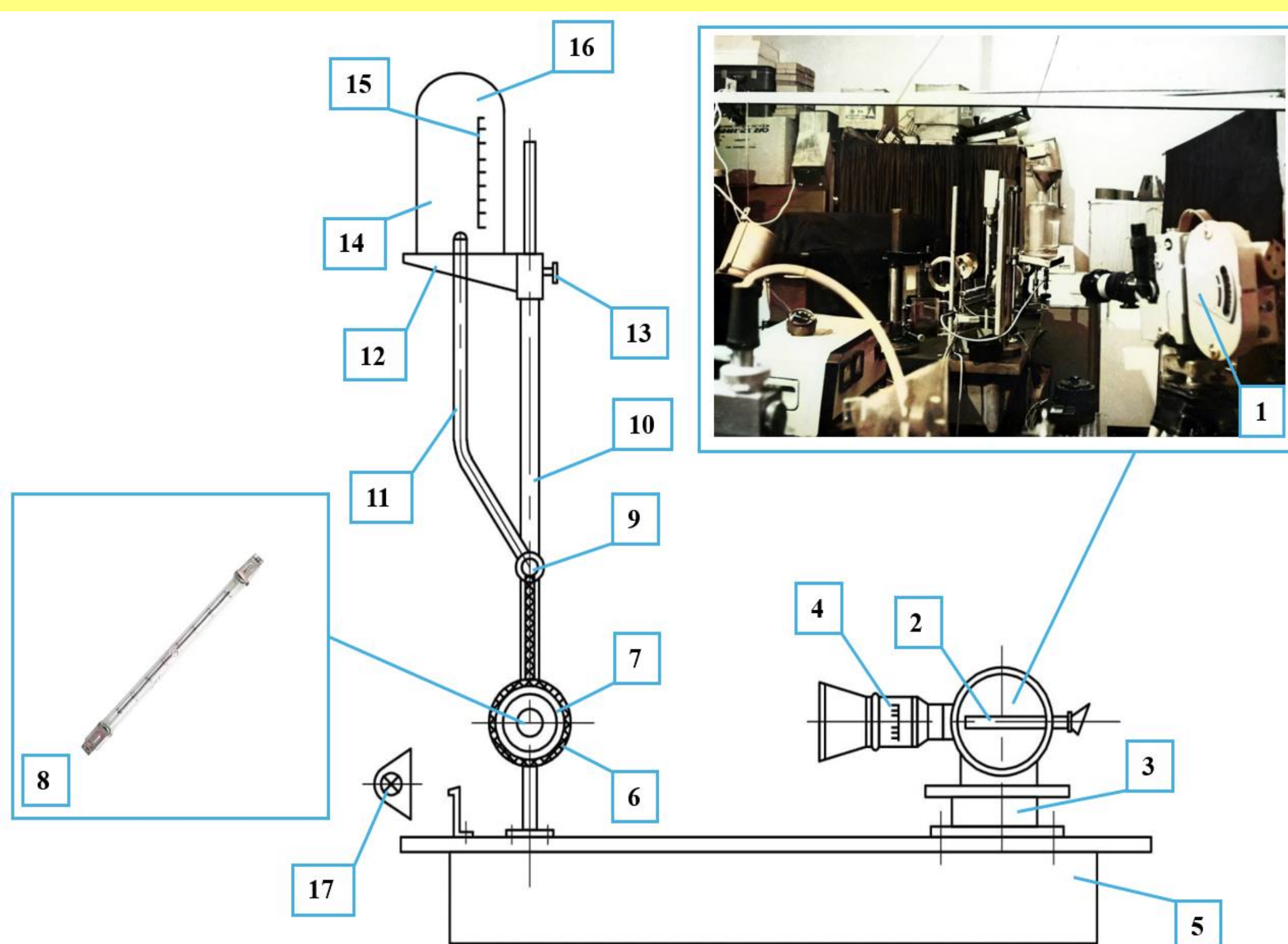


Fig. 1. Schematic diagram of the high-speed cinematography test setup.

Observations were conducted at heat flux densities of $q = 40, 67, 94,$ and 120 kW/m^2 , as well as at intermediate values of q . Critical heat loads were investigated, and dynamic operating modes of the system under extreme conditions were recorded photographically, after which liquid was re-supplied to the artery.

For the 0.14×0.4 mesh structure, liquid supply against the direction of gravitational forces was also studied.

Recording was carried out after the establishment of a steady thermal regime, which typically took 5–7 minutes.

COOLING SYSTEM OF STATOR NOZZLE VANES

The system is presented in the form of a ring (a heat pipe with a capillary-porous structure), the inner part of which acts as an evaporator and is adjacent to the nozzles, while the outer part serves as a condenser cooled by a secondary coolant (Fig. 2).

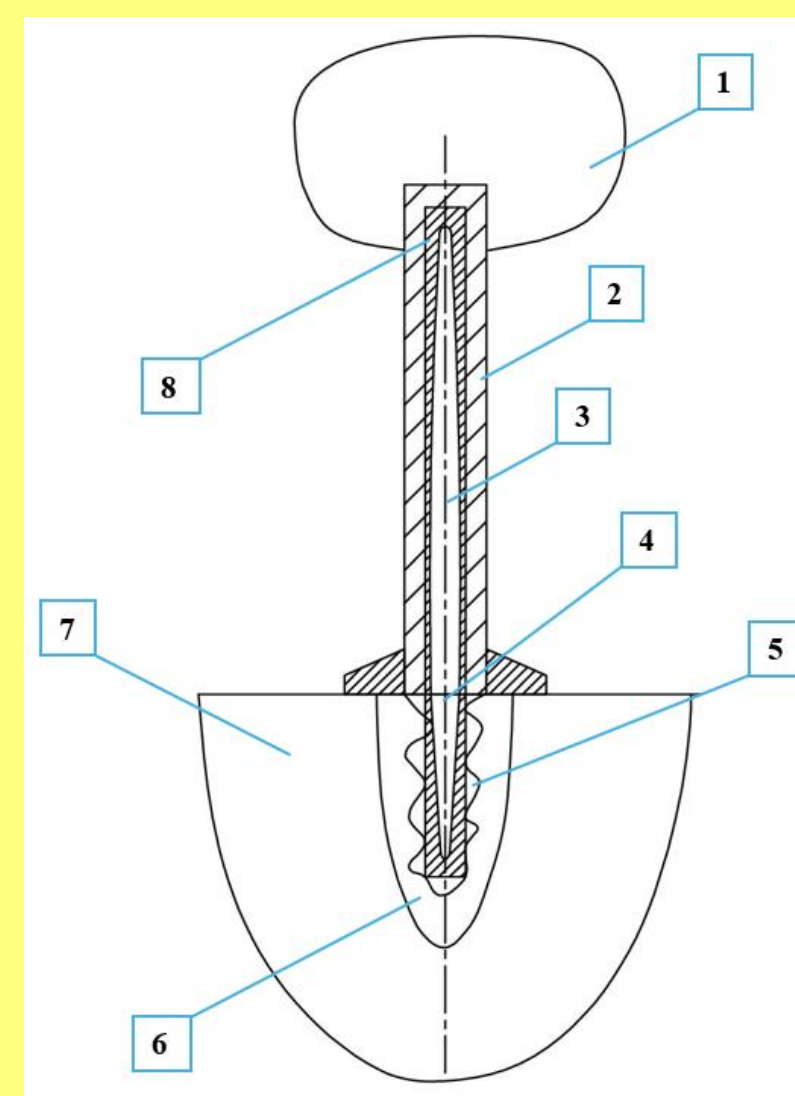


Fig. 2. Schematic diagram of the closed evaporation-condensation cooling system for stator nozzle vanes

The notation in Fig. 2 is as follows: 1 – diaphragm rim, 2 – airfoil section of the vane, 3 – blind channels in the vane, 4 – cooling channels in the diaphragm body, 5 – heat sink radiator, 6 – primary coolant (steam), 7 – diaphragm body, 8 – capillary-porous structure.

Results

During turbine startup and shutdown, bubble nucleation and collapse give rise to cumulative phenomena which, together with corrosion and electrochemical processes, destroy the stress concentrator (nucleation site), bringing it to the size of a critical crack.

The resulting erosion process may thus be accompanied by mechanical impact, cavitation, and electrochemical corrosion. In the event of instantaneous vapor concentration within a cavity (pit), its volume collapses instantaneously, generating a powerful cumulative effect - cavitation (Fig. 3). Shock waves propagate into the bulk of the turbine components, promoting the development of fatigue cracks through which oxygen ingress occurs.

Fig. 3 presents cinematograms of heat and mass transfer processes: *a* - for a 0.14×0.4 wick; *b* - for a 0.4 wick at $q = 40 \div 120 \text{ kW/m}^2$; *c* and *d* - for a 0.4 wick at enlarged scale at $q = 94 \text{ kW/m}^2$, $n = 0.14$, and varying liquid excess ratio $m = m_l / m_v = 14(m_l \text{ and } m_v - \text{liquid and vapor flow rates})$.

As bubble development progresses, destruction of capillary low-temperature coatings occurs, both of natural and artificial origin.

A cavity formed in the structure coating under the combined action of several phenomena - impact, cavitation, and corrosion - leads to erosion and degradation of rotor and stator components.

The greater the penetration depth of the thermal wave or the size of the disintegrating particles of the porous coating [1], the longer the time required for component failure.

As the turbine ramps up to its rated (or part-load) operating mode, the heat fluxes at the machine surface stabilize and converge toward their mean integral design values.

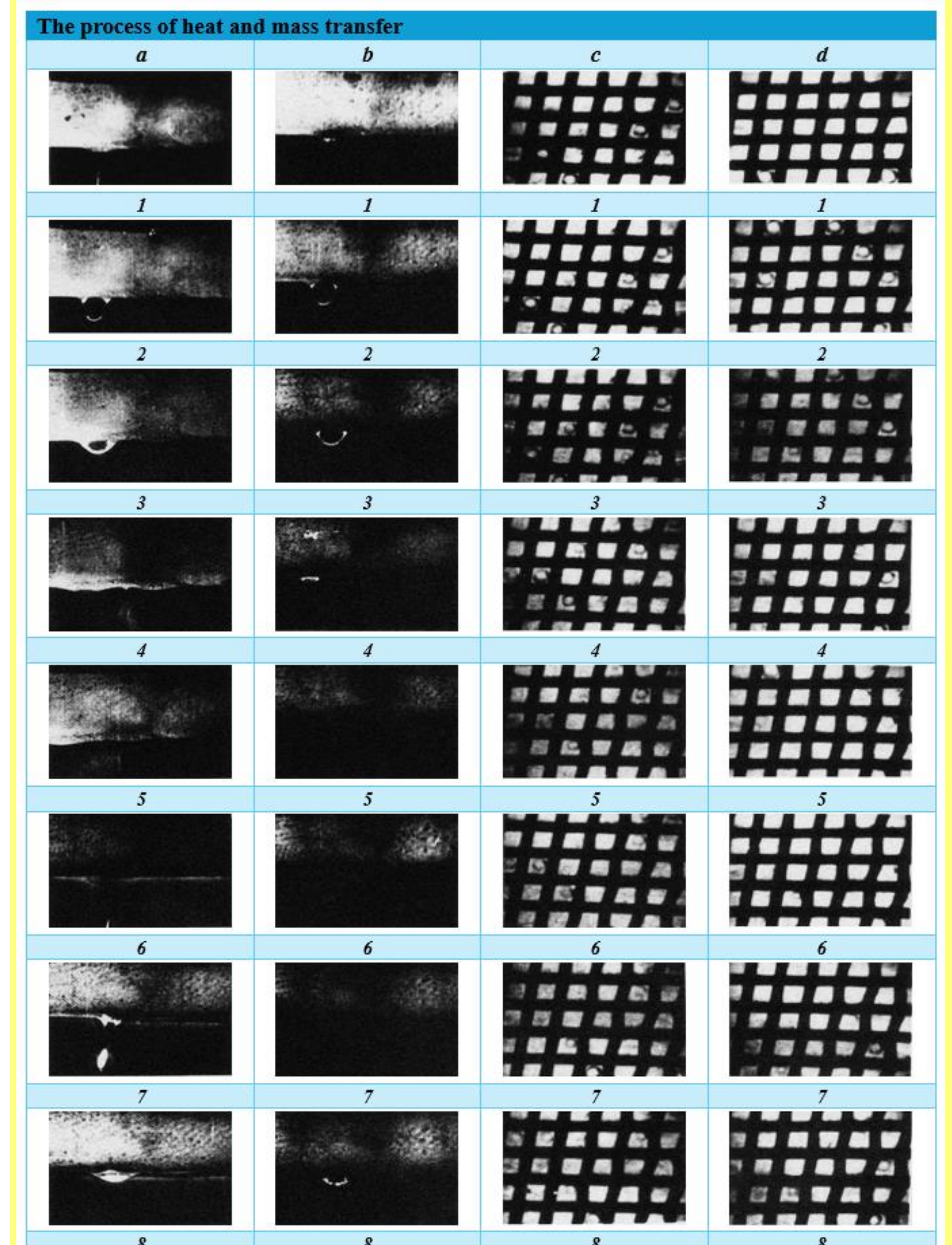


Fig. 3. Cinematograms of heat and mass transfer processes for various wicks, heat loads, and liquid excess ratios.

Conclusions

1. Experimental setups for optical investigation methods have been developed. The results of experimental data processing are presented in the form of liquid droplet ejection and the dynamics of vapor and liquid phase development under various heat transfer conditions (structure type, parameters q, m, τ).

2. A cooling method for steam turbine nozzles operating at non-standard supercritical parameters has been developed. A closed evaporation-condensation cooling system for the nozzles and inter-vane passage of a turbine stage, implemented as a wick structure or coating, has been investigated.

3. A mesh cell hydraulic diameter of 0.15×10^{-3} m and a structure thickness of 0.75×10^{-3} m have been selected. Analysis of phase transformations on the heat transfer surface revealed their dominant role in the explosive behavior of the vapor phase, giving rise to cumulative and cavitation effects.

4. The investigated cooling system is an attractive alternative to heat-resistant alloys, improving equipment reliability. The conducted studies are based on optical methods proven effective for predicting equipment service life.

References

- [1] Genbach, A.A. et al. Boiling crisis in porous structures. Energy. 2022, 259, 125076. <https://doi.org/10.1016/j.energy.2022.125076>
- [2] Ge, M. Recent Developments and Future Directions in Flow Visualization: Experiments and Techniques. Fluids. 2025, 10, 23. <https://doi.org/10.3390/fluids1002023>
- [3] Javan, A. Population Inversion and Continuous Optical Maser Oscillation in a Gas Discharge Containing a He-Ne Mixture. Phys. 1961. <https://doi.org/10.1103/PhysRevLett.6.106>
- [4] Svelto, O. Principles of Lasers, Fourth edition, Springer, 1998. <https://doi.org/10.1007/978-1-4757-6266-2>
- [5] Val'shin, A.M., et al. Increase in the power of a commercial He-Ne laser under combined pumping. Phys. Wave Phen. 23, 199–201 (2015). <https://doi.org/10.3103/S1541308X15030061>